Size-Shape Relationships in the Mesozoic Planispiral Ammonites

Authors: Parent, Horacio, Greco, Andrés F., and Bejas, Matías

Source: Acta Palaeontologica Polonica, 55(1) : 85-98

Published By: Institute of Paleobiology, Polish Academy of Sciences

URL: https://doi.org/10.4202/app.2009.0066

Size-shape relationships in the Mesozoic planispiral ammonites

HORACIO PARENT, ANDRÉS F. GRECO, and MATÍAS BEJAS

Parent, H., Greco, A.F., and Bejas, M. 2010. Size-shape relationships in the Mesozoic planispiral ammonites. *Acta Palaeontologica Polonica* 55 (1): 85–98.

Ammonites are of outstanding importance in dating events of the Mesozoic and in the study of mechanisms, modes and timing of evolutionary processes. These applications rely on a detailed understanding of their morphology and the modes of variation. It has been known for a long time that their shape is composed of a number of highly correlated features. A new model, called the ADA-model, is introduced for the study of shell morphology (size and shape). The new model is based on classic dimensions which are stable parameters throughout ontogeny, giving very close agreement between predictions and actual observations. It was applied in the exploration of the morphospace occupied by the planispirally coiled and the regularly uncoiled Mesozoic Ammonoidea, based on two new reduced morphospaces introduced for the analysis. Results obtained expose close relationships between size and shape, and general patterns in the ammonite shell morphology and morphogenesis. (i) The relative apertural height of the whorl section relative to the diameter of the shell (H_2/D) is involved in definition of size and shape. (ii) This same dimension shows a strong tendency to be $H_2/D = 0.3$. (iii) There are some geometrically possible shell shapes (or morphotypes) which seem to have not been developed since they are not known in the current record. Assuming the known ranges of protoconch size and whorl number as constraints, the ADA-model strongly suggests that these morphotypes have not been developed for the too large or too small sizes the shells would have attained, well outside of the actual size range of the planispirally coiled Ammonoidea. (iv) The law of covariation is shown to be a general pattern within the planispiral ammonites which describes structured variation of the shell shape. (v) A large fraction of the non-structured variation seems originate in the lack of correlation between the relative umbilical diameter and width of the whorl section.

Key words: Ammonoidea, size, shell shape, dimensionless analysis, reduced morphospaces, new model, Mesozoic.

Horacio Parent [parent@fceia.unr.edu.ar], Lab. Paleontología, Universidad Nacional de Rosario, Pellegrini 250, 2000 Rosario, Argentina;
Andrés F. Greco [agreco@fceia.unr.edu.ar] and Matías Bejas [bejas@ifir-conicet.gov.ar], Departamento de Física and Instituto de Física de Rosario, CONICET, Universidad Nacional de Rosario, Pellegrini 250, 2000 Rosario, Argentina.

Received 5 June 2009, accepted 27 October 2009, available online 29 October 2009.

Introduction

Ammonites (Cephalopoda: Ammonoidea) are very abundant marine fossils with a vast record worldwide. They are unique in possessing two valuable attributes: 1) they are the most precise geological clocks for the Mesozoic Era (see Callomon 1995, 2001) and, 2) each individual specimen preserves the whole shell ontogeny, from the embryonic chamber or protoconch up to the terminal adult border or peristome (Bassé 1952; Arkell et al. 1957). These outstanding properties enable the use of ammonites in the chronology of the Mesozoic to be coordinated with the study of the ontogeny and evolution under fine control of the essential property of evolving systems, the time. Ammonites could be the model fossil organism par excellence for studies in the framework of Evolutionary Developmental Biology (Evo-Devo).

Nevertheless the combination of these properties has not been easy to manage, mainly because of the wide spectra and complexity of the patterns of horizontal (intraspecific) and vertical (evolutionary) variation. The understanding of these patterns is based on the knowledge of the form and meaning of relationships between the dimensions and between size and shape. After inspection of a major part of the large number of papers which include some kind of statistical description, it is evident that there are general patterns of strong correlation between sets of dimensional features during growth. This morphologic integration is associated with the patterns of variation of the dimensions. Indeed, some relative dimensions are strongly variable within a single species, especially the width of the whorl section (e.g., Sturani 1971; Callomon 1985; Dagys and Weitschat 1993; Parent 1998). Other features are stable during growth and between individuals of a single species, especially the maximum relative height of the whorl section (see Parent 1998: 104; Parent and Greco 2007; and discussion below). The widely accepted "laws of covariation" (see Buckman 1892; Westermann 1966; Hammer and Bucher 2005 for recent review and references) are other indicators of the existence of structure in the variation of shell shape beyond the notoriously wide ranges of intraspecific and transpecific variability.

doi:10.4202/app.2009.0066

In spite of the wide ranges of variability it is commonly held that ammonites had few shape features or characters for producing innovations. This seems to be in accord with the wide recurrence of homoeomorphies. These limitations, or constraints, for producing shape innovations are in contrast with the richness in sculpture. Thus, homoeomorphies may be successfully resolved by considering the ontogeny of shape and sculpture. The fact that ammonites have produced an apparently restricted part of the "available morphology" which may be generated from a coiled cone, has been studied by several authors (e.g., Raup 1967; Ward 1980; Dommergues et al. 1996). These studies were mostly based on the dimensions and/or variables proposed by Raup (1961, 1966), or few others like whorl section perimeter (Ubukata et al. 2008). Nevertheless, these models need especially suited specimens and, moreover, they are not written in terms of the standard dimensions which are used in every systematic description (see e.g., Enay 1966). Therefore these interesting studies are hardly related to the standard and always essential taxonomic descriptions and systematic studies.

Adult size and shape-at-size of ammonites are also widely variable, even within a single species, recalling what is in living coleoids widely recognised as a characteristic trait of their natural history (see e.g., Boyle and Boletzky 1996). Size is one of the most readily impressive features of an object under observation but, however, may be important or not depending on the circumstantial interest. In classification the relative, intragroup size is meaningful if some degree of isomorphism exists between the organisms grouped. Thus, size-shape relationships are crucial in classification. When these relationships are considered there may be obtained not only robust natural classifications but also additional causal or phenomenological information of the organism considered.

In the present paper we introduce a model using classical dimensions for the study of relationships between size and shape, morphogenetic rules and structure of the variation of shell morphology. The model is compared with actual ammonites, using a large sample of data which can be assumed representative of, at least, the largest part of the planispiral Mesozoic Ammonoidea. Results obtained from the analysis of size and shape are discussed stressing the value of dimensionless analysis and size-shape relationships.

Institutional abbreviations.—LPB, Laboratorio de Paleontología, Universidad Nacional de Rosario, Rosario, Argentina; MOZ-PI, Museo Prof. Olsacher, Dirección Provincial de Minería de Neuquén, Zapala, Argentina.

Other abbreviations.—A, vector or morphologic space; a_1, a_2, constants; c, constant; Ca, cadicone; $C_V(\%)$, percentual coefficient of variation (%); D, diameter of the shell; D_{pro}, protoconch diameter; e, Euler number; H_1, whorl section height; H_2, whorl section apertural or ventral height; λ, constant; m, constant; n, sample size; N_w, whorl number; Ox, oxycone; Pl, platycone; $<Q>$, arithmetic mean of a variable Q; r, Pearson coefficient of correlation; RM, reduced morphologic space; s, standard deviation; Se, serpenticone; Sp, spherocone; t, constant; θ, variable; U, umbilical diameter; W, whorl section width.

Material and method

Material.—Material used for this study belongs to 201 species of Triassic, Jurassic, and Cretaceous planispirally coiled and regular-uncoiled representatives of the order Ammonoidea Zittel, 1884 (suborders Ceratitina, Phylloceratina, Lytoceratina, Ammonitina, and Ancyloceratina), distributed in time as shown in Fig. 1A. 1003 specimens were measured with several transversal (different specimens) and longitudinal (ontogeny of a single specimen) subsamples producing a large sample of 1222 sets of measurements for shell diameter $D \geq 3$ mm. Most of the specimens are adults or subadults, mainly with their body chamber. The information was obtained from laboratory measurements and literature (see Appendix 1). Sampling was designed to include most of the wide variety of morphotypes known within the planispiral Ammonoidea. Representativeness of our large sample within the Ammonoidea is hard or impossible to quantify, mainly because the very large numbers of nominal genera and species described. Nevertheless, it can be seen in Fig. 1A that the temporal distribution of number of species for each series of the Mesozoic is rather even, and also the number of species for each of the defined morphotypes of the classification below (see Fig. 1B). The only exception is the cadiconic morphotype which is scarce in our samples but probably in close proportion to its occurrence in the actual spectrum of the Mesozoic Ammonoidea.

Conventions.—We have adopted a concept of morphology with two components, separable under certain circumstances: shape and size. Shape is described by dimensionless variables (proportions between dimensions) of the shell, irrespective of the size. This latter consists of dimensional variables (metric dimensions) as defined below. Sculpture (ribs, tubercules, constrictions) is not considered in this study. Measurements are taken between ribs and if the specimen is keeled, the keel is considered a part of the morphology. Sculptural elements like ribs and tubercles are considered outgrowths which do not contribute to size dimensions in continuous form as do the keel. Size dimensions used are linear distances as defined in Fig. 2. These dimensions or variables define a multidimensional vector or morphospace $A[5] = (D, U, W, H_1, H_2)$. Shell morphology is decomposed for analysis in two subsets corresponding to the classical lateral and apertural views, as used in figuring specimens since the earliest authors: (i) morphology in the equatorial or coiling plane (lateral view) $A[4]_1 = (D, U, H_1, H_2)$ and (ii) morphology in the transversal plane (apertural view) $A[4]_2 = (D, W, H_1, H_2)$. For shape analysis these dimensions are used in the form of dimensionless quantities or shape variables: U/D, H_1/D, W/D, H_2/D, and H_2/H_1. These quantities can be considered measurements of shape or relative morphol-

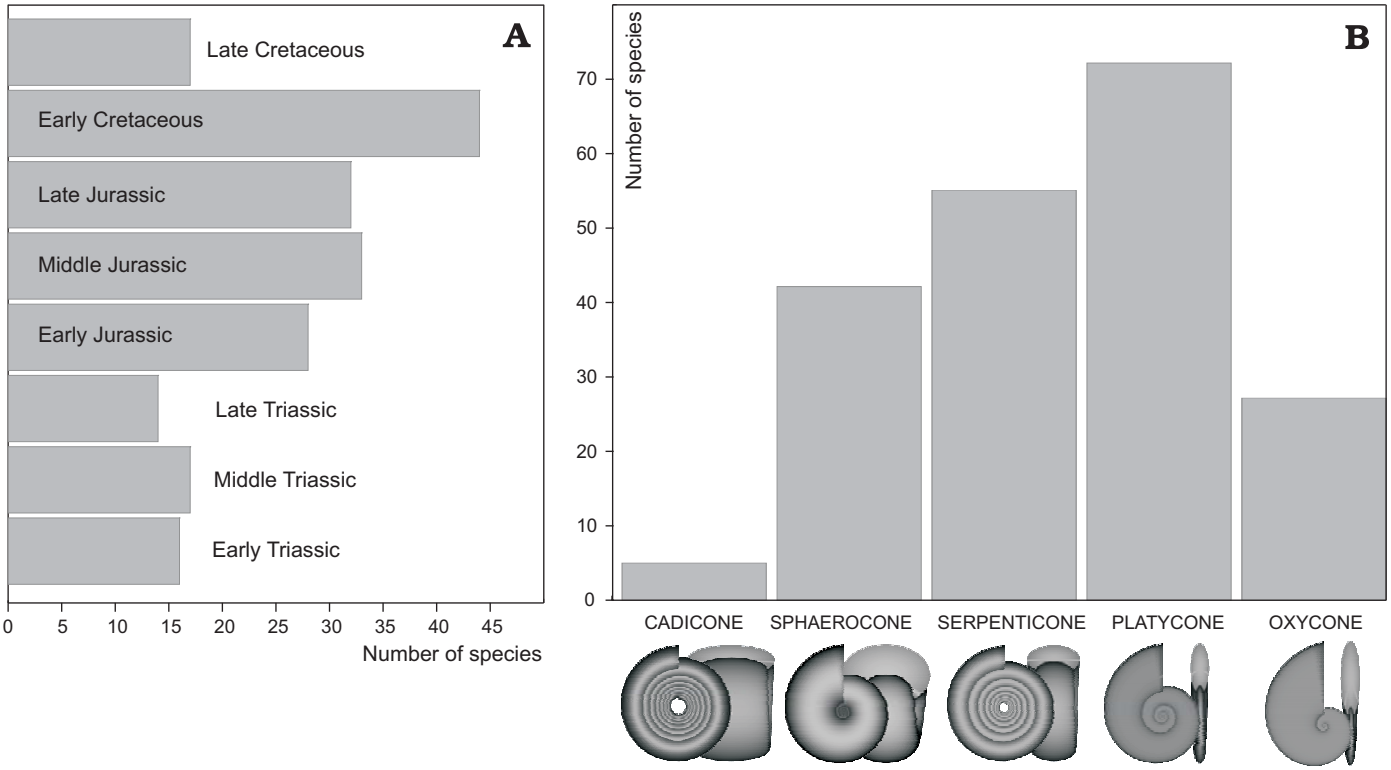

Fig. 1. Representativity of the studied sample in time and shape diversity. **A**. Number of species considered for each subdivision of the Mesozoic. **B**. Number of species for each morphotype as defined in text. Some species include individuals belonging to different morphotypes of the adopted classification.

ogy, instantaneous character states (Parent 1997), irrespective of any growth model or pattern. Thus, they may be used for comparison between different ammonites in the similar ontogenetic stages at different sizes, for the size component of morphology is removed. Additionally for analysis of size the whorl number (N_w) computed from the end of the protoconch onwards, and the protoconch diameter (D_{pro}) are considered. The broadest ranges adopted are: $D_{pro} = (0.2, 1.05)$ mm (based on data in Landman et al. 1996), and $N_w = (5, 9)$ for adult ammonites (based on data in Makowski 1963 and Bucher et al. 1996).

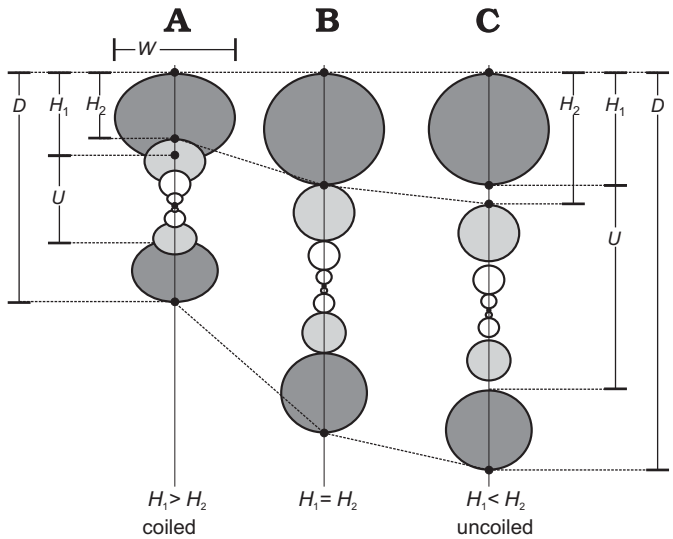

Fig. 2. Dimensions measured in coiled and uncoiled ammonites. Note the transposition between H_1 and H_2 from coiled (**A**) to uncoiled (**C**) ammonites, passing through the identity between H_1 and H_2 in the singular case (**B**).

Our data-matrix is not suitable for statistical inferences due to the heterogeneity originated in the diversity of sources of the information contained. This condition is not crucial in the phenomenological and geometrically based approach adopted for the present study. However, where pertinent, essential statistical measurements or parameters are provided: arithmetic mean of a variable Q is denoted $\langle Q \rangle$, the percentual coefficient of variation $C_V(\%) = 100\ s / \langle Q \rangle$ (being s the standard deviation), the Pearson coefficient of correlation r, and the sample size n.

Shell shape morphotypes.—Shape diversity of planispiral ammonites arises from a combination of different whorl section shapes and involution degrees. This variety is herein classified in a few morphotypes based on a simplification of that of Westermann (1996). Although inevitably subjective as any classification of this kind, it is useful for presentation and discussion of results. Regular uncoiled ammonites fall widely in the classical gyrocone shape but we have included them in serpenticones or platycones, so that coiled and regular-uncoiled ammonites are not discriminated in this classification (see Fig. 1B):

– Oxycone (Ox): involute to moderately evolute lenticular shell, flanks converging into a narrow or acute venter; whorl section subtriangular, typically higher than wide.
– Platycone (Pl): involute to uncoiled, discoidal shell, flanks

doi:10.4202/app.2009.0066

parallel to subparallel, narrow to moderately wide venter; commonly higher than wide whorl section.
- Serpenticone (Se): evolute to uncoiled, rounded or flattish flanks, venter rounded, commonly wide. Whorl section rounded, subrounded or subrectangular.
- Sphaerocone (Sp): involute, globular to subglobular shell, whorl section typically rounded and wider than high.
- Cadicone (Ca): whorl section wider than high, depressed, evolute and widely umbilicate.

Some species include individuals belonging to different morphotypes of this classification (intraspecific variation). On the other hand, in most species, individuals change between different morphotypes during ontogeny. Thus, otherwise indicated, comparisons are mainly based on adult individuals or at comparable diameter and/or developmental stage.

Results

The ammonite shape in the equatorial plane: the ADA-model.—Let us start with the usual logarithmic spiral model and consider the curve generated by $r(\theta) = c \cdot e^{\lambda\theta}$ where c and λ are constants (Fig. 3A). On this curve is placed an ellipse with center on the curve. The plane of the ellipse is perpendicular to the curve, and the radii are $a_1(\theta) = 2m \cdot e^{\lambda\theta}$ and $a_2(\theta) = t \cdot a_1^{\lambda\theta}$, where m and t are constants.

These equations include constants (c, λ, m) which are very hard or impossible to obtain by direct measurement of specimens, and, on the other hand, they have no meaning in morphological terms. Differently to other developments (see Introduction and Discussion below) we propose here the following re-parameterisation. For a given number of whorls (N_w), i.e., for a given angle θ, the following relationships are obtained (see Fig. 3B):

$$U(\theta) = D(\theta) - H_1(\theta) - H_1(\theta - \pi)$$

$$H_2(\theta) = r(\theta) + a_1(\theta) - [r(\theta - 2\pi) + a_1(\theta - 2\pi) = (c+2m)(1-e^{-2\pi\lambda})e^{\lambda\theta},$$

and

$$D(\theta) = r(\theta) + a_1(\theta) + r(\theta - \pi) + a_1(\theta - \pi) = (c+2m)(1+e^{-\pi\lambda})e^{\lambda\theta}$$

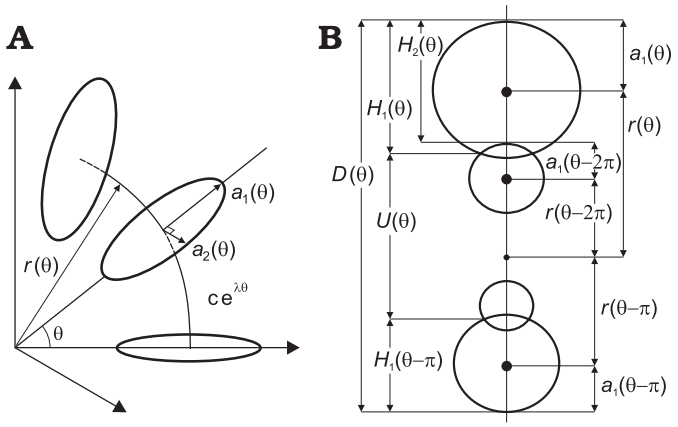

Fig. 3. **A**. Representation of the log-spiral and the associated ellipse representing the whorl section. **B**. Geometric equivalences between variables of the log-spiral and classical variables defined in Fig. 2.

It can be seen that the dependance on θ for $D(\theta)$ and $H_2(\theta)$ is only through $e^{\lambda\theta}$, and the same is true for $H_1(\theta)$. Using the above equations and $\frac{H_2}{D} = 1 - e^{-\lambda\pi}$, it is obtained:

$$\frac{U}{D} = 1 - 2\frac{H_1}{D} + \left(\frac{H_1}{D}\right)^2 \frac{H_2}{H_1} \quad (1)$$

Equation 1 is written in terms of the classical variables or dimensions D, H_1, H_2, U (as defined in Fig. 2) which, moreover, are standard in the sense that they are easily interpreted visually and used in almost every description of ammonites. Note that for $H_2/H_1 = 1$, which is a singular case (see Fig. 2B), Equation 1 becomes $\frac{U}{D} = \left(1 - \frac{H_1}{D}\right)^2$, which corresponds to the starting point of the phenomenological derivation approached formerly in Parent and Greco (2007). This singular case is seen in some few ammonites, typically some Lytoceratids. When the degree of involution is $H_2/H_1 < 1$, it leads to a reduction of U/D as a consequence of the involution. It is quite evident that Equation 1 is also valid for uncoiled ammonites with dimensions defined in Fig. 2. It is worth to note that the reduction of U/D due to the involution term in Equation 1 arises by analytical derivation from the logarithmic spiral model, but not phenomenologically introduced.

Equation 1 is presented in terms of dimensionless quantities. It is clear from dimensional analysis (Bridgman 1949) that H_1/D and H_2/H_1 are independent variables, even if H_1 is represented in both of them. On the other hand, Equation 1 is a mathematical derivation from the logarithmic spiral model by means of a change of a set of independent variables to another set of independent variables. This model is hereafter called ADA-model for adimensional ammonite.

Following the spirit of Parent and Greco (2007) we consider Equation 1 as an "equation of state". Like in the case of an ideal gas, where temperature, pressure and volume are not free to take any value but they are related by an equation of state, a given ammonite, in a given state of growth, has its variables (U, D, H_1, H_2) connected by Equation 1. In the mentioned paper (Parent and Greco 2007) it was pointed out, widely supported by empirical observations, that H_1/D and H_2/H_1 tend to be strongly stable for a given species throughout the post-nepionic ontogeny. In the context of the ADA-model this fact is not an assumption. Indeed, following the derivation of Equation 1 it can be seen that H_1/D and H_2/H_1 are constants, independently of the number of whorls, for a given model parameter, showing that the model is consistent with observations. Thus, the averages $\langle H_1/D \rangle$ and $\langle H_2/H_1 \rangle$ may be considered representative numbers of the species.

After computing these two mean values for a given species, we then computed an estimated value $(U/D)_{pred}$ by means of Equation 1 for comparison. In the next section the validity of the model is evaluated as the matching between estimates produced by Equation 1 and actual values.

Agreement between estimates of the ADA-model and actual values.—The accuracy with which Equation 1 represents

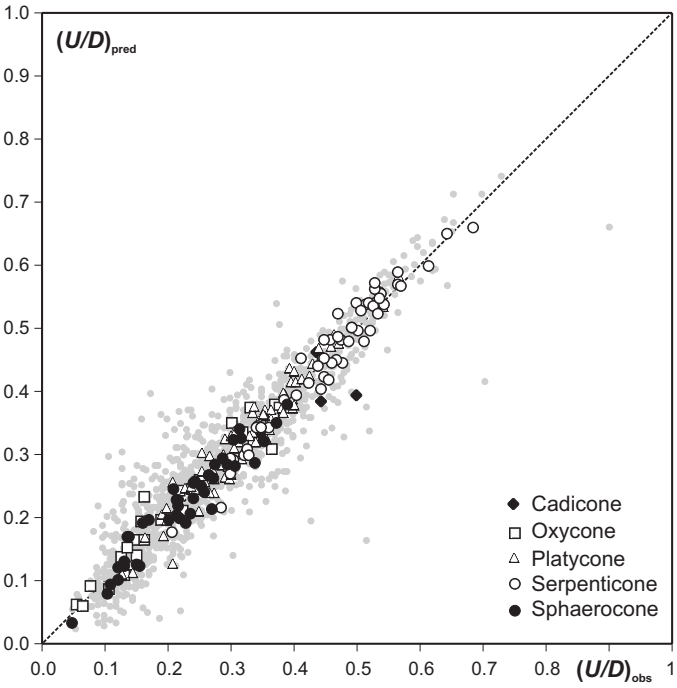

Fig. 4. Correlation between actual and estimated (Equation 1) values of U/D for all the ammonites studied ($N = 1222$; gray points) and mean values for each species classified by morphotypes. The line corresponding to $(U/D)_{obs} = (U/D)_{pred}$ is shown for comparison.

actual ammonites was tested by means of a simple evaluation consisting of a comparison between estimated values of U/D, denoted by $(U/D)_{pred}$, and actual sample values. Actual values were obtained from the species average of individual values of U/D and are denoted by $<U/D>_{obs}$. The relative error between predictions and observations was calculated for each species as $\varepsilon(\%) = 100\cdot[|(U/D)_{pred} - <U/D>_{obs}|]/ <U/D>_{obs}$ (see Appendix 1). A simple inspection of the relative errors shows that they are relatively low, through the range 0–46% ($n = 201$ species) with an average of 7% (90% of estimates concentrate within the interval 0–15%). The analysis of the model, as explained below, gives additional support to this assumption. The good agreement is also clearly reflected in the high correlation ($r = 0.98$, significant at $P < 0.01$) between $(U/D)_{pred}$ and $<U/D>_{obs}$ as shown in Fig. 4. The predicted U/D obtained for each individual measurement ($N = 1222$) are also plotted in Fig. 4 with light shaded circles, showing that correlation between predictions and observations is also very high ($r = 0.93$, significant at $P < 0.01$). These significant, strong correlations give additional support to the use of mean values for each species for proceeding analysis.

These results show that Equation 1 is not only a good estimator, but also robust and stable (irrespective of the way it is evaluated). Indeed, it captures relevant features of the ammonite shell shape, a significant part of the whole shape and its variation between and within species and ontogenetic stages, no matter the morphotype considered. It is assumed that this stability is based on a strong tendency of the ammonite shell in maintaining the proportions H_1/D and H_2/H_1 rather invariable, independently of the size or ontogenetic stage of the individuals. In summary, a given species with its characteristic H_1/D and H_2/H_1, will tend to have a constant value of U/D. It follows that these quantities are well represented by their averages, thus supporting that they are independent.

The reduced morphologic space (H_2/H_1 – H_1/D).—The simplicity and reliability of Equation 1 provide for a framework for searching structural and functional relationships between morphological features of the ammonite shell, going beyond a simple multivariate description.

The model indicates that H_1/D and H_2/H_1 are relevant variables, enough for describing the ammonite shape in the equatorial plane. Therefore, it seems natural to introduce the

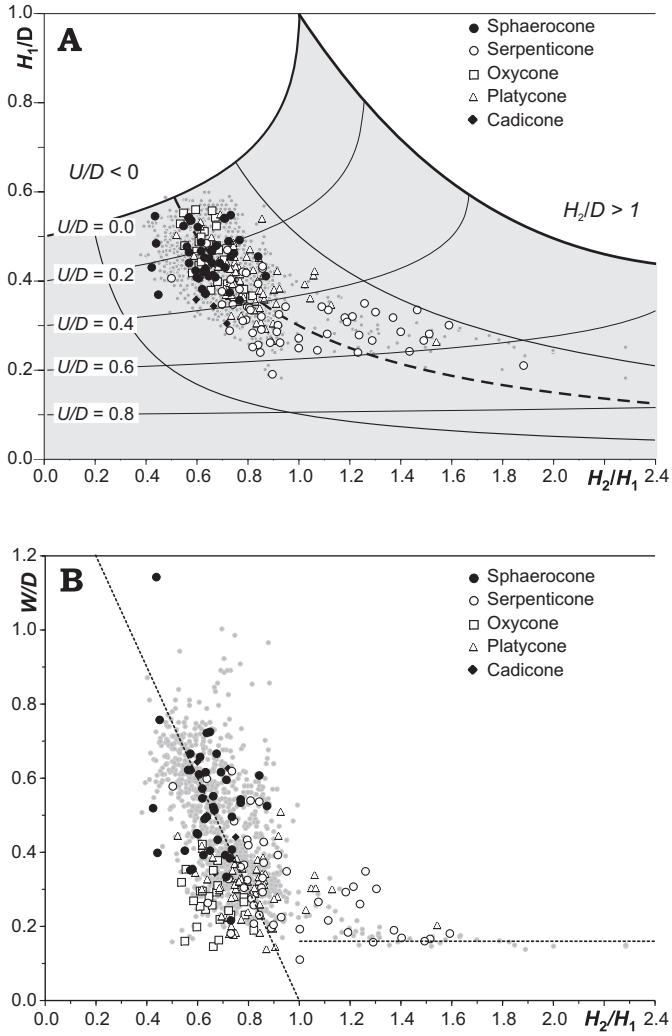

Fig. 5. **A**. Reduced morphospace RM_1. Plot of individual measurements (gray points, $N = 1222$) and mean values for the 201 species studied classified by morphotypes. The theoretical iso-U/D curves are explained in text. The gray trapezoid-like area is delimited by curves as explained in text. The bold broken curve shows the main trend $H_1/D = 0.3/(H_2/H_1)$. The two thinner curves [$H_1/D = 0.5/(H_2/H_1)$ and $H_1/D = 0.1/(H_2/H_1)$] delimit the constrained empirical morphospace CM_1, the portion of RM_1 realised or occupied by Mesozoic ammonoids. **B**. Reduced morphospace RM_2 with plots of individual measurements ($N = 1222$) in gray points, and mean values of each one of the 201 species studied. The general trend is represented by two straight lines as described in the text.

doi:10.4202/app.2009.0066

reduced morphospace $RM_1 = (H_2/H_1, H_1/D)$. Since each species is closely characterised by its corresponding averages $\langle H_2/H_1 \rangle$ and $\langle H_1/D \rangle$, they are represented by a point in RM_1. In Fig. 5A each of the studied species is located showing well defined and consistent trends. The distribution is such that ammonites with similar shape, following the adopted classification, tend to cluster in rather well defined portions of RM_1. Sphaerocones are well separated in the scatter from serpenticones. Oxycones tend to cluster partially overlapping sphaerocones, while platycones tend to overlap with serpenticones. Nevertheless, the separation of platycones from oxycones is not as clear as in the case of sphaerocones and serpenticones.

Additional information can be obtained from the family of curves for constant *U/D*, which will be called iso-*U/D* curves. Using Equation 1 it can be shown that these curves are defined by the following equation:

$$\frac{H_1}{D} = \left(\frac{H_2}{H_1}\right)^{-1} + \sqrt{\left(\frac{H_2}{H_1}\right)^{-2} - \left(1 - \frac{U}{D}\right)}\left(\frac{H_2}{H_1}\right)^{-1}.$$

A set of selected iso-*U/D* curves are depicted in Fig. 5A. The iso-$U/D = 0.3$ is nearly the threshold separating oxycones and sphaerocones from platycones and serpenticones. Cadiconic ammonites tend to cluster rather independently, with low values of both H_1/D and H_2/H_1, below the iso-$U/D = 0.3$. The differential clustering of the morphotypes points to a well structured morphospace (H_2/H_1, H_1/D), meaning that the overall morphology is well characterised by these shape variables. Individual observations also follow the same patterns of distribution that the species average, as shown by gray points in Fig. 5A. These patterns give additional support to Equation 1 which is based on these variables. As a corollary, it is interesting to note that the negligible variation of *U/D* through wide ranges of H_2/H_1, as shown by the iso-*U/D* curves, shows that H_2/H_1 is a direct measurement of the degree of involution of the shell.

The geometrically possible shell shapes define a theoretical morphospace with well defined boundaries. The iso-$U/D = 0$ separates regions with $U/D < 0$ and $U/D > 0$ (Fig. 5A). Clearly, $U/D < 0$ has no meaning for the ammonites studied herein. This "empty" region of RM_1 is predicted from Equation 1. Within the family of iso-*U/D* curves the limit given by $U/D = 1$ (the *x*-axis) is the boundary out of which the umbilicus should be larger than the diameter. Other boundary or threshold curve is indicated with a thick solid line in the top right of Fig. 5A; it has the hyperbolic form $H_1/D = 1/(H_2/H_1)$, that is $H_2 = D$, outside which $H_2 > D$. Finally, the theoretical ammonite-morphospace becomes trapezoid-like by a fourth curve: $H_2/H_1 = 0$ (the *y*-axis) where $H_2 = 0$. Note that just a single, negligible observation out of 1222 falls outside of RM_1.

The theoretical region of RM_1 (Fig. 5A) brings about the natural question of why only a small portion is actually represented by Mesozoic ammonites (see Introduction). This very interesting question can be discussed in the framework of the ADA-model. Evidently there are intrinsic and extrinsic constraints operating in shell construction which are not included in Equation 1, which is mainly geometrical and does not contain parameters yielding additional information, in explicit form, about such factors. Nevertheless the geometrical constraints can be worked out and importantly, their implications and origin can be outlined with confidence as discussed below.

Mesozoic ammonites are concentrated in RM_1 approximately between two hyperbolae: $H_1/D = 0.5/(H_2/H_1)$, and $H_1/D = 0.1/(H_2/H_1)$ as shown in Fig. 5A. The centre of gravity can be roughly described by the hyperbola $H_1/D = 0.3/(H_2/H_1)$ where a main trend is clearly evident (bold dashed line in Fig. 5A). It may be interpreted as that, in average, the apertural height of the whorl section tends to be $H_2 = 0.3D$. This trend is strongly supported by the plot of observations of H_2/D versus *D*. The scatter is relatively tightly concentrate around $\langle H_2/D \rangle = 0.303$ as indicated by $C_V(\%) = 20\%$, $n = 1222$ (Fig. 6A).

The dimension *D* may be defined geometrically as a function of the whorl number N_w, the protoconch size D_{pro} : $D(\theta = 0)$ and the rate of diameter growth H_2/D as

$$D = D_{pro}\left(1 - \frac{H_2}{D}\right)^{-2N_w}.$$

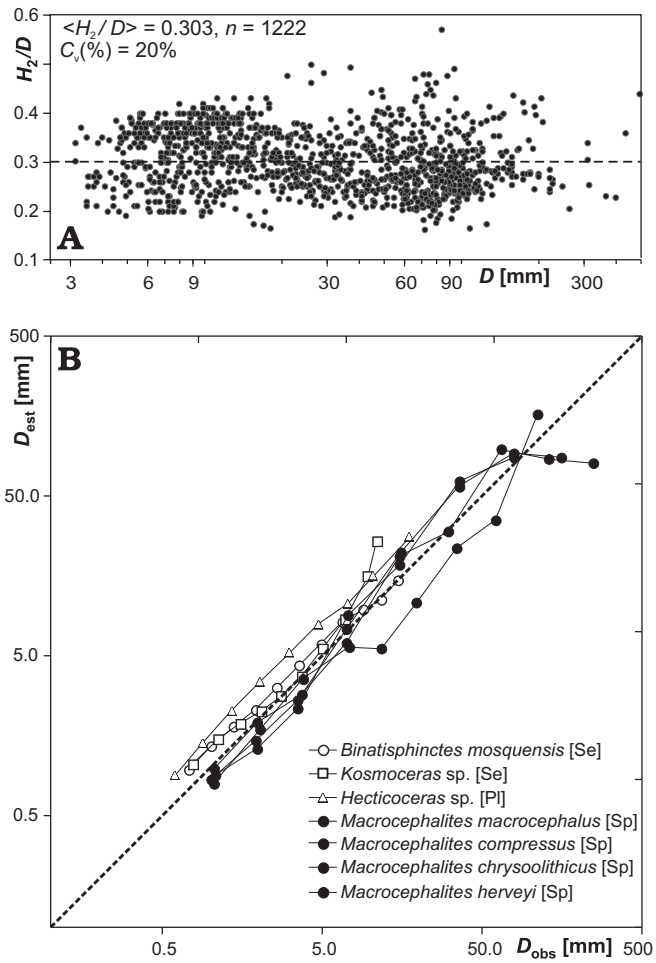

Fig. 6. **A**. Plot of all individual measurements ($n = 1222$) of H_2/D versus *D* showing relatively low variation in the Mesozoic Ammonoidea. The main trend $H_2/D = 0.3$ is almost equal to the average $\langle H_2/D \rangle = 0.303$. **B**. Comparison of estimations of *D* versus actual measurements through the ontogeny of selected specimens (see Appendix 1 for details of material).

Fig. 6B shows, for selected cases, that the correlation between D_{obs} and D_{est} is high ($r = 0.80$, $n = 63$, significant at $P < 0.01$).

Below the curves $U/D < 0$ and $H_2 = D$, any shape is geometrically possible within RM_1. Nevertheless, as indicated above, only a relatively small part of RM_1 is represented by Mesozoic ammonites. It is possible to show (for a fixed D_{pro} and N_w) that ammonites, above the hyperbole $H_1/D = 0.5/(H_2/H_1)$ should be 10^3 to 10^6 times larger in size (D) than those nearby the main trend $H_1/D = 0.3/(H_2/H_1)$. In contrast, ammonites well below the hyperbole $H_1/D = 0.1/(H_2/H_1)$ should be 10^{-2} to 10^{-3} times smaller in size than those nearby the main trend. For example, an ammonite having $H_2/H_1 = 1.2$ and $H_1/D = 0.60$, well above the hyperbole $H_1/D = 0.5/(H_2/H_1)$, should have a size $D = 67523$ mm, considering the lowermost known values of $D_{pro} = 0.2$ mm and $N_w = 5$. On the other hand, an ammonite having $H_2/H_1 = 0.2$ and $H_1/D = 0.10$ [well below the hyperbole $H_1/D = 0.1/(H_2/H_1)$] should have a size $D = 1.5$ mm, considering the uppermost known values of $D_{pro} = 1.05$ mm and $N_w = 9$. Even considering that most ammonites undergo ontogenetic changes of H_2/D during growth, well above or below the main trend, these figures are valid for they were calculated assuming the mentioned actual extreme values of D_{pro} and N_w.

Considering the broad assumption $H_2 = 0.3D$ and the extreme values of D_{pro} and N_w, it may be estimated that adult ammonites should range within the interval $D = 7$ mm (for $D_{pro} = 0.2$ mm, and $N_w = 5$) to $D = 645$ mm (for $D_{pro} = 1.05$ mm, and $N_w = 9$). These estimations are no more than a main theoretical range and, however, might be very close to the range of adult sizes actually known. Indeed, the large sample used in the present study is well included in that theoretical interval, ranging between $D = 10$ mm and $D = 495$ mm. However, special cases of adult ammonites that are close to or exceed these extreme values are well known (e.g., Sturani 1971; Kennedy and Cobban 1976, 1990; Stevens 1985; Torrens 1985).

Another important outcome of the above analysis is related to the size increments during growth. The rate of overall size increase after addition of a complete whorl during growth is $D[N_w+1]/D[N_w] = (1-H_2/D)^{-2}$. For example, the main trend $H_2/D = 0.3$ defines a pattern of doubling size for each whorl added during growth. However, the variability of growth rate has practical importance when comparing different specimens during classification, as can be seen with ammonites which almost double their size each half a whorl ($H_2/D = 0.42$). The taxonomic significance of size differences between morphologically similar specimens must be carefully assessed in order to avoid attributing excessive taxonomic value to differences in size. This is especially important for those ammonites with high H_2/D at least in the last whorls, for there is no evidence suggesting that the number of whorls of the ammonite shell should be a constant, even within a single species.

The ammonite shape in the transversal plane.—In spite of attempts to include the dimension W in a single equation for describing both the equatorial and transversal planes, no satisfactory results were obtained. However, the fact that the largest part of the morphology of the ammonite shell is described by Equation 1 independently of W/D, indicates that the influence of this latter on U/D could likely be small or negligible. This fact suggests independence during morphogenesis between W/D and shape in the equatorial plane as discussed previously (Parent and Greco 2007). This apparent non-correlation between U/D and W/D is well illustrated by three examples taken from our large sample (Fig. 7): *Quenstedtoceras lamberti*, *Poecilomorphus cycloides*, and *Dactylioceras clevelandicum*. In these three monospecific samples of equal size specimens, U/D varies very little and irrespective of the widely variable W/D. Respectively the correlations are $r[U/D, W/D] = 0.21$ ($n = 6$), -0.63 ($n = 6$) and -0.98 ($n = 3$), the three cases are statistically insignificant (Student's t test). The large sample (gray points in Fig. 7) has $r[U/D, W/D] = -0.38$ which is also statistically insignificant.

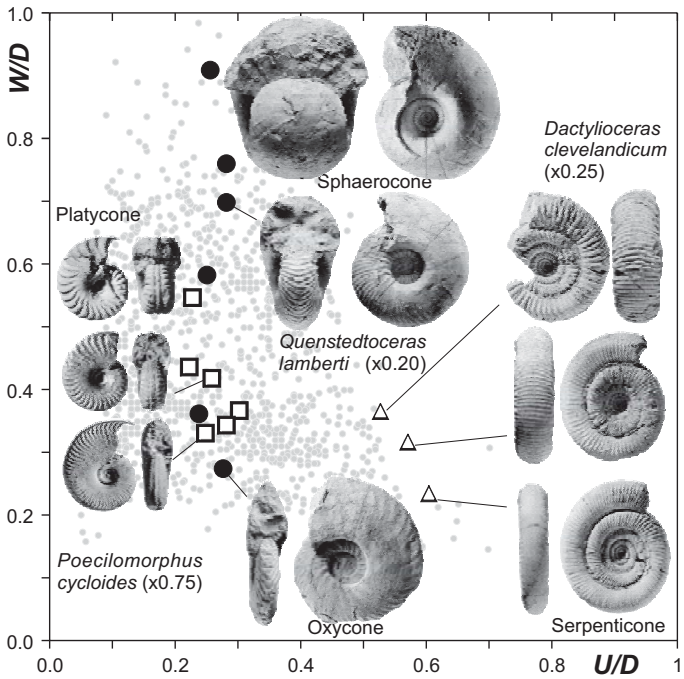

Fig. 7. Plot of W/D versus U/D for the whole large sample (gray points), $n = 1222$. Three samples are selected to show the almost invariable relative umbilical width along significant variation of relative width of whorl section. White squares: *Poecilomorphus cycloides* (Middle Jurassic) modified from Sturani (1971: pl. 8); black circles: *Quenstedtoceras lamberti* (Middle Jurassic) modified from Callomon (1985: fig. 5b); and white triangles: *Dactylioceras clevelandicum* (Early Jurassic) modified from Howarth (1973: pls. 3, 4).

The widely observed "law of covariation" is very accurately illustrated by the plot of W/D versus H_2/H_1 shown in Fig. 5B. This trend is closely followed by our sample assumed representative of the Mesozoic Ammonoidea as a whole, by which it can be considered a general trend. The trend arises from the negative correlation between W/D and H_2/H_1 mentioned above, which allows to define a second reduced morphologic space $RM_2 = (H_2/H_1, W/D)$. Considering that W/D is strongly correlated with the involution degree as measured by

doi:10.4202/app.2009.0066

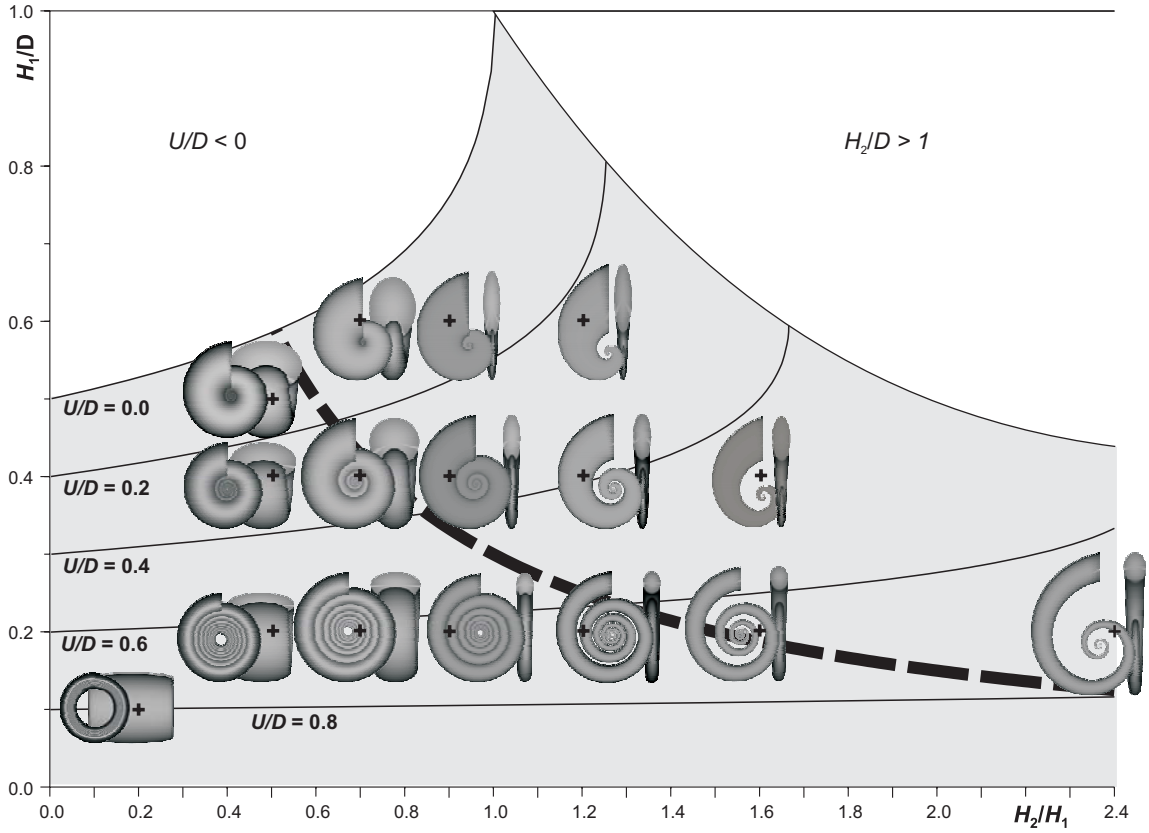

Fig. 8. ADA-model simulated ammonites (as explained in text) showing the distribution of morphotypes in the reduced morphologic space RM_1. All ammonites are scaled to nearly equal size. Extreme morphotypes (out of the constrained morphospace CM_1, see Fig. 5A) not known within the Mesozoic Ammonoidea are shown side-by-side with known morphotypes for comparison. Bold broken line is the main trend $H_2 = 0.3D$.

H_2/H_1 but directly neither with H_1/D nor U/D, the morphogenetic link between the shape of the ammonite in the equatorial and transversal planes appears to be H_2/H_1. The trend in RM_2 may be approximately described by the phenomenological relationship $W/D = (3/2) - (3/2)\,(H_2/H_1)$ if $H_2 < H_1$ and $W/D = 0.18$ if $H_2 > H_1$ as depicted in Fig. 5B by dashed lines. This equation is, undoubtedly, a gross approximation but is simple and, importantly, follows the general trend observed including the interesting phenomenon consisting of roughly invariant W/D for $H_2 > H_1$ (uncoiled ammonites).

Discussion and conclusions

The range of shell-shapes actually developed by planispiral ammonites within the wide geometrically available spectrum of RM_1 and RM_2 is rather narrow, and follows the relationships closely represented by the ADA-model. Our results seem to clearly indicate that the constraints which have limited the spectrum of actual morphologies into a sector of RM_1 (Fig. 5A) are related or conjugated in the size D.

Results obtained from exploration of the distribution of ammonite morphological variety in RM_1 and RM_2 may be summarised as follows.

The shape can be described by H_2/H_1, H_1/D and W/D. The two latter dimensionless quantities are strongly correlated with, and decreasing along, increments of H_2/H_1. U/D may be considered a function of H_1/D and H_2/H_1.

The dimensionless H_2/D, although not directly impressive to the eye, is the more influential in shape and size. Indeed, it is involved in definition of both aspects of morphology, the shape and the size (as diameter growth rate). There is a strong general tendency in the planispirally coiled Ammonoidea to follow the relationship $H_2 = 0.3D$ (Fig. 5A). On the other hand, H_2/H_1 is the link between the shape in the equatorial plane (lateral view) and the shape in the transversal plane (apertural view).

Mathematically size limits imply constraints between protoconch diameter (initial condition), shell shape and whorl number as shown by the equation presented above. There are some geometrically possible shell shapes (or morphotypes) which seem to have not been developed since they are not known in the available fossil record. Assuming the known ranges of D_{pro} and N_w as constraints, the ADA-model strongly suggests that these morphotypes have not been developed for the too large or too small sizes the shells would have attained, well outside of the actual size range of the planispirally coiled Ammonoidea. In other words, within the known range of D_{pro} there are certain shell shapes which would have generated too large ammonites after a very low number of whorls. Conversely, other kind of unrealised shell shapes would have generated too small ammonites after a very high number of

whorls. Too large and too small mean well beyond the known range of size in actual ammonites. This proposed order of the causal relationships between the mentioned variables or features is not the only which could be conceived, but in our view it is the most plausible.

The correlation between *W/D* and *U/D* is very low and statistical insignificant. This low correlation should be the main source of non-structured, intra- and transpecific variation in the ammonite shell. This non-structured variation may be hard to separate from the structured variation (that which arises from covariation between shape traits). Discrimination between structured and not-structured variation has a crucial role in recognition of morphological continuity or discontinuity within samples as the main morphological criterium for tracing limits between species.

The negative covariation between the relative width of whorl section *W/D* and involution H_2/H_1 is demonstrated to be not only a pattern of intraspecific variation but also a general trend for the Mesozoic coiled ammonoids as a whole, as far as represented by our sample. This pattern is classically described under the law of covariation. It was shown above that the degree of involution of the shell is best described by the proportion H_2/H_1. Under this consideration the law of covariation seems to be more generally valid in the form: evolute (high H_2/H_1)-compressed-finely ribbed, towards the opposite pole: involute (lower H_2/H_1)-stout, depressed (wide whorl section)-coarsely ribbed. In this form the pattern is tighted to the components of shape which are correlated, thus producing well structured variation. Covariation is manifested in coiled ammonites, those in which the successive whorls are in dorso-ventral contact each other. In uncoiled ammonites the relative whorl width *W/D* is always lower, and, moreover, tending to be almost constant along increasing H_2/H_1 (Fig. 5B).

Fig. 8 shows different simulated ammonites corresponding to different exact locations in RM_1. This picture also includes some morphotypes unknown within the Ammonoidea. These computer-simulations are obtained from Equation 1 and using the approximation for *W/D* proposed above. The simulations are not in scale but their relative sizes can be easily obtained from Fig. 5A and the equation for calculation of *D* given above. Drawings were made with Blender (version 2.42a; free access at www.blender.org) using a rather simple computer program written in the Python language (free version 2.4). The obtained figures are very real in outer shape, but they are based on perfectly elliptical whorl sections and isometric ontogenies which are not found in any actual ammonite.

Finally, it may be noted that some previous studies of ammonite morphology based on geometrical models (e.g., Raup 1967) have similarities with the presented in this paper. Nevertheless, there is no room for comparison since direct conversions between classical variables of A[5] = (D, U, W, H_1, H_2) and those used by Raup (1966, 1967) have not been explored. However, Raup (1967) has made some of the earliest attempts to explain the "morphospace occupation patterns" in Palaeozoic and Mesozoic ammonoids.

Acknowledgements

Armin Scherzinger (Hättingen, Germany), Victor Schlampp (Schwanstetten, Germany) and Michal Zatoń (University of Silesia, Sosnowiec, Poland) for loaning some of the studied ammonites or information and measurements. John C.W. Cope (University of Cardiff, Cardiff, UK) has kindly enhanced the langauge style of the manuscript. Adriana Foussats (Universidad Nacional de Rosario, Rosario, Argentina) for useful suggestions. Øyvind Hammer (University of Oslo, Oslo, Norway) and a further anonymous reviewer gave us valuable suggestions for enhancing the present paper.

References

Aguirre-Urreta, M.B. 1985. Ancylocerátidos (Ammonoidea) aptianos de la Cordillera Patagónica Austral, Provincia de Santa Cruz, Argentina. *Boletín de la Academia Nacional de Ciencias, Córdoba* 56: 135–257.

Aguirre-Urreta, M.B. and Rawson, P.F. 1999. Lower Cretaceous ammonites from the Neuquén Basin, Argentina: *Viluceras*, a new Valanginian subgenus of *Olcostephanus*. *Cretaceous Research* 20: 343–357. doi:10.1006/cres.1999.0154

Arkell, W. J., Kummel B., and Wright, W.C. 1957: Mesozoic Ammonoidea. *In*: R.C. Moore (*ed.*): *Treatise on Invertebrate Paleontology: Part 1, Mollusca 4*, L80–L437. Kansas University Press, Lawrence.

Bassé, E. 1952. Sous-classe des Ammonoidea. *In*: J. Piveteau (coord.), *Traité de Paléontologie, tome 2*, 522–555. Masson et Cie, Paris.

Bloos, G. 2004. Psiloceratids of the earliest Jurassic in the North-West European and Mediterranean Provinces—remarks and new observations. *Stuttgarter Beiträge zur Naturkunde* B347: 1–15.

Boyle, P.R . and Boletzky, S. v. 1996. Cephalopod populations: definition and dynamics. *Philosophical Transactions of the Royal Society of London B* 351: 958–1002. doi:10.1098/rstb.1996.0089

Branger, P., Nicolleau, P., and Vadet, A. 1995. *Les ammonites et les oursins de l'Oxfordien du Poitou*. 149 pp. Musées de la ville de Niort and APGP Poitou-Charentes-Vendée, Niort.

Bridgman P.W. 1949. *Dimensional Analysis*. Yale University Press, New Haven.

Bucher, H. 1994. New ammonoids from the Taylori Zone (Middle Anisian, Middle Triassic) from Northern Nevada (USA). *Mémoires de Géologie (Lausanne)* 22: 1–8.

Bucher, H., Landman, N.H., Klofak, S.M., and Guex, J. 1996: Mode and Rate of Growth in Ammonoids. *In* N.H. Landman, K. Tanabe, and R.A. Davis (eds.), Ammonoid Paleobiology. *Topics in Geobiology* 13: 407–461.

Buckman, S.S. 1887–1907. *A Monograph of the Ammonites of the Inferior Oolite Series*. 456 pp. Palaeontographical Society, London.

Burckhardt, C. 1927. Cefalópodos del Jurásico Medio de Oaxaca y Guerrero. *Boletín del Instituto Geológico y Minero de México* 47: 1–106.

Callomon, J.H. 1985. The evolution of the Jurassic Ammonite family Cardioceratidae. *Special Papers in Palaeontology* 33: 49–90.

Callomon, J.H. 1995. Time from fossils: S.S. Buckman and Jurassic high-resolution geochronology. *In*: M.J. Le Bas (ed.), Milestones in Geology. *Geological Society of London Memoir* 16: 127–150.

Callomon, J.H. 2001. Fossils s geological clocks. *In*: C.L.E. Lewis and S.J. Knell (eds.), The Age of the Earth from 4004 BC to AD 2002. *Geological Society of London Special Publication* 190: 237–252.

Cobban, W.A. 1988a. *Tarrantoceras* Stephenson and related ammonoid genera from Cenomanian (Upper Cretaceous rocks in Texas and the Western Interior of the United States. *United States Geological Survey Professional Paper* 1473: 1–30.

Cobban, W.A. 1988b. The Late Cretaceous ammonite *Spathites* Kummel and Decker in New Mexico and Trans-Pecos Texas. *New Mexico Bureau of Mines & Mineral Resources Bulletin* 114: 5–21.

Cobban, W.A. and Kennedy, W.J. 1989. The Ammonite *Metengonoceras*

doi:10.4202/app.2009.0066

Hyatt, 1903, from the Mowry Shale (Cretaceous) of Montana and Wyoming. *United States Geological Survey Bulletin* 1787: L1–L11.

Dagys, A.S. 2001. The ammonoid family Arctohungaritidae from the Boreal Lower–Middle Anisian (Triassic) of Arctic Sea. *Revue de Paléobiologie* 20: 543–561.

Dagys, A.S. and Weitschat, W. 1993. Extensive intraspecific variation in a Triassic ammonoid from Siberia. *Lethaia* 26: 113–121. doi:10.1111/j.1502-3931.1993.tb01801.x

Delanoy, G. 1992. Les ammonites du Barremien Supérieur de Saint-Laurent de L'Escaréne (Alpes Maritimes, Sud-Est de la France). *Annales du Muséum d'Histoire Naturelle de Nice* 9: 1–148.

Dietl, G. 1978. Die heteromorphen Ammoniten des Dogger. *Suttgarter Beiträge zur Naturkunde B* 33: 1–97.

Dietze, V., Chandler, R.B., and Callomon, J.H. 2007. The Ovale Zone (Lower Bajocian, Middle Jurassic) at Little Down Wood (Dundry Hill, Somerset, SW England). *Stuttgarter Beiträge zur Naturkunde B* 368: 1–45.

Dommergues, J.-L. 1987. L'evolution chez les Ammonitina du Lias moyen (Carixien, Domerien basal) en Europe occidentale. *Document des Laboratoires de Géologie de la Faculté des sciences de Lyon* 98: 1–297.

Dommergues, J.L., Laurin, B., and Meister, C. 1996. Evolution of ammonoid morphospace during Early Jurassic radiation. *Paleobiology* 22: 219–240.

Enay, R. 1966. L'Oxfordien dans la moitié sud du Jura français. *Nouvelles Archives du Museum d'Histoire naturelle de Lyon* 8: 1–624.

Giovine, A.T.Y. 1950. Algunos cefalópodos del Hauteriviense de Neuquén. *Revista de la Asociación Geológica Argentina* 5 (2): 35–76.

Giovine, A.T.Y. 1952. Sobre una nueva especie de *Crioceras*. *Revista de la Asociación Geológica Argentina* 7 (1): 71–75.

Gulyaev, D.B. 2001. Infrazonal Ammonite scale for the Upper Bathonian–Lower Callovian of Cental Russia. *Stratigaphy and Geological Correlation* 9: 65–92.

Haas, O. 1955. Revision of the Jurassic ammonite fauna of Mount Hermon, Syria. *Bulletin of the American Museum of Natural History* 108: 1–210.

Hammer, Ø. and Bucher, H. 2005. Buckman's first law of covariation—a case of proportionality. *Lethaia* 38: 1–6. doi:10.1080/00241160510013196

Howarth, M.K. 1973. The stratigraphy and ammonite fauna of the Upper Liassic grey shales of the Yorkshire Coast. *Bulletin of the British Museum (Natural History) Geology* 22: 237–278.

Imlay, R.W. 1960. Early Cretaceous (Albian) Ammonites from the Chitina Valley and Talkeetna Mountains, Alaska. *United States Geological Survey Professional Paper* 354D: 1–114.

Joly, B. 2000. Les Juraphyllitidae, Phylloceratidae, Neophylloceratidae (Phylloceratacea, Phylloceratina, Ammonoidea) de France au Jurassique et au Crétacé. *Geobios Mémoire Spécial* 23: 1–204.

Jones, D.L. 1967. Cretaceous ammonites from the lower part of the Matanuska Formation Southern Alaska. *United States Geological Survey Professional Paper* 547: 1–49.

Kemper, E. and Wiedenroth, K. 1987. Klima und Tier-Migrationen am Beispiel der frühkretazischen Ammoniten Nordwestdeutschlands. *Geologisches Jahrbuch* A96: 315–363.

Kennedy, W.J. and Cobban, W.A. 1976. Aspects of Ammonite biology, biogeography, and biostratigraphy. *Special Papers in Paleontology* 17: 1–94.

Kennedy, W.J. and Cobban, W.A. 1988. The Late Cretaceous ammonite *Romaniceras* Spath, 1923, in New Mexico. *New Mexico Bureau of Mines & Mineral Resources Bulletin* 114: 23–34.

Kennedy, W.J. and Cobban W.A., 1990. Cenomanian micromorphic ammonites from the Western Interior of the USA. *Palaeontology* 33: 379–422.

Kennedy, W.J., Landman, N.H., Cobban, W.A., and Scott, G.R. 2000. Late Campanian (Cretaceous) heteromorph ammonites from the Western Interior of the United States. *Bulletin of the American Museum of Natural History* 251: 1–88. doi:10.1206/0003-0090(2000)251<0001:LCCHAF>2.0.CO;2

Kummel, B. 1972. The Lower Triassic (Scythian) Ammonoid *Otoceras*. *Bulletin of the Museum of Comparative Zoology Harvard University* 143: 365–417.

Landman, N.H., Tanabe, K., and Davis, R.A. 1996: Ammonoid Paleobiology. *Topics in Geobiology* 13: 1–845.

Makowski, H. 1963. Problem of sexual dimorphism in ammonites. *Palaeontologia Polonica* 12: 1–92.

Meister, C. 1986. Les ammonites du Carixien des Causses (France). *Mémoires suisses de Paléontologie* 109: 1–209.

Meister, C. 1989. Les ammonites du Crétacé supérieur d'Ashaka, Nigeria. *Bulletin des centres de recherches exploration-production Elf Aquitaine* (Supplemente) 13: 1–84.

Mitta, V.V. and Starodubtseva, I.A. 2000. W.A. Stchirowsky and study of the Mesozoic in Alatyr-Kumysh area (basin of the Middle Volga) [in Russian]. *Vernadsky Museum-Novitates* 5: 1–20.

Murphy, M.A. 1967. Aptian and Albian Tetragonitidae (Ammonoidea) from Northern California. *University of California Publications in Geological Sciences* 70: 1–43.

Pandey, D.K. and Callomon, J.H. 1995. The Middle Bathonian ammonite families Clydoniceratidae and Perisphinctidae from Pachchham Island. *Beringeria* 16: 125–145.

Parent, H. 1997. Ontogeny and sexual dimorphism of *Eurycephalites gottschei* (Tornquist) of the Andean lower Callovian (Argentine-Chile). *Geobios* 30: 407–419. doi:10.1016/S0016-6995(97)80201-X

Parent, H. 1998. Upper Bathonian and lower Callovian ammonites from Chacay Melehué (Argentina). *Acta Palaeontologica Polonica* 43: 69–130.

Parent, H. and Greco, A.F. 2007. An "Equation of state" fro the morphology of Jurassic ammonites: a multidimensional law based on classical dimensions. *Revue de Paleobiologie* 26: 41–53.

Patrulius, D. and Avram, E. 1976. Les céphalopodes des couches de Carhaga (Tithonique supérieur–Barrémien inférieur). *Mémoires Institut de Géologie et de Geophysique* 24: 153–201.

Pavia, G. 1983. Il genere *Ptychophylloceras* Spath, 1927 (Ammonoidea, Phylloceratacea) nel Baiociano sudeuropeo. *Atti della Accademia Nazionale dei Lincei, série 8*, 17: 5–31.

Rakus, M. and Guex, J. 2002. Les ammonites du jurassique inférieur et moyen de la dorsale tunisienne. *Memoires de Géologie (Lausanne)* 39: 1–217.

Raup, D.M. 1961. The geometry of coiling in gastropods. *Proceeding of the National Academy of Sciences USA* 47: 602–609. doi:10.1073/pnas.47.4.602

Raup, D.M. 1966. Geometric analysis of shell coiling: general problems. *Journal of Paleontology* 40: 1178–1190.

Raup, D.M. 1967. Geometric analysis of shell coiling: coiling in Ammonoids. *Journal of Paleontology* 41: 43–65.

Riccardi, A.C. 1983. Kossmaticeratidae (Ammontina) y nomenclatura estratigráfica del Cretácico Tardío en Lago Argentino, Santa Cruz, Argentina. *Ameghiniana* 20: 317–345.

Ropolo, P. and Salomon, M. 1992. Evolution du déroulement – Passage du stade criocératique au stade subaspinocératique ou protacriocératique – chez les certains populations d'ammonites hétéromorphes de l'Hauterivien moyen (zones à Nodosoplicatum et à Sayni). *Géologie Méditerranéenne* 19: 189–227.

Ropolo, P. and Gonnet, R. 1995. Nouveaux exemples de dimorphisme chez les Ancyloceratina (Ammonoidea) de l'Hauterivien vocontien. *Géologie Méditerranéenne* 22: 93–109.

Rulleau, L. 1997. *Perilytoceras* nov. gen. (Lytoceratina), du Toarcien supérieur de la Province NW Européenne. *Geobios Mémoire Spécial* 20: 451–461.

Rulleau, L., Bécaud, M., and Neige, P. 2003. Les ammonites traditionnellement regroupées dans la sous-famille des Bouleiceratinae (Hildoceratidae, Toarcien): aspect phylogénétiques, biogéographiques et systématiques. *Geobios* 36: 317–348. doi:10.1016/S0016-6995(03)00034-2

Schlatter, R. 1980. Biostratigraphie und Ammonitenfauna des Unter-Pliensbachium in typusgebiet (Pliensbach, Holzmaden und Nürtingen; Württemberg, SW-Deutschland). *Stuttgarter Beiträge zur Naturkunde B* 65: 1–261.

Sprey, A.M. 2002. Early ontogeny of three Callovian ammonite genera (*Binatisphinctes, Kosmoceras* and *Hecticoceras*) from Ryazan (Russia). *Abhandlungen der Geologischen Bundesanstalt* 57: 225–255.

Stevens, G.R. 1985. A revision of the Lytoceratinae (Subclass Ammonoidea) including *Lytoceras taharoaense* n. sp., Upper Jurassic, New Zealand. *New Zealand Journal of Geology and Geophysics* 28: 153–185.

Sturani, C. 1971. Ammonites and stratigraphy of the "Posidonia alpine" beds of the Venetian Alps (Middle Jurassic, mainly Bajocian). *Memorie degli Instituti di Geologia e Mineralogia dell'Universitá di Padova* 28: 1–190.

Tavera, J.M. 1985. *Los ammonites del Tithonico Superior – Berriasiense de la Zona Subbética (Cordilleras Béticas)*, 1–381. Tésis de la Universidad de Granada, Granada.

Taylor, D.G. and Guex, J. 2002. The Triassic/Jurassic System boundary in the John Day Inlier, east-central Oregon. *Oregon Geology* 64: 3–28.

Thierry, J. 1978. Le genre *Macrocephalites* au Callovien inferieur (Ammonites, Jurassique moyen). *Mémoires Géologiques de l'Université de Dijon* 4: 1–491.

Torrens, H.S. 1985. The biology of ammonites. *The Journal of the Open University Geological Society* 6: 17–21.

Tozer, E.T. 1994. Canadian Triassic Ammonoid faunas. *Geological Survey of Canada Bulletin* 467: 1–663.

Ubukata, T., Tanabe, K., Shigeta, Y., Maeda, H., and Mapes, R. 2008. Piggyback whorls: A new theoretical morphologic model reveals constructional linkages among morphological character in ammonoids. *Acta Palaeontologica Polonica* 53: 113–128.

Urlichs, M. 2006. Dimorphismus bei *Ceratites* aus dem Germanischen Oberen Muschelkalk (Ammonoidea Mitteltrias) mit Revision einiger Arten. *Stuttgarter Beiträge zur Naturkunde B* 363: 1–85.

Ward, P. 1980. Comparative shell shape distribution in Jurasic–Cretaceous ammonites and Jurassic–Tertiary nautilids. *Paleobiology* 6: 32–43.

Westermann, G.E.G. 1966. Covariation and taxonomy of the Jurassic ammonite *Sonninia adicra* (Waagen). *Neues Jahrbuch für Geologie und Paläontologie, Abhandlungen* 124: 289–312.

Westermann, G.E.G. 1996. Ammonoid Life and Habitat. *In*: N.H. Landman, K. Tanabe, and R.A. Davis (eds.), Ammonoid Paleobiology. *Topics in Geobiology* 13: 607–707.

Zakharov, Y.D. and Shkolnik, E.L. 1994. Permian–Triassic cephalopod facies and global phosphatogenesis. *Mémoires de Géologie (Lausanne)* 22: 171–182.

Zatoń, M. 2008. Taxonomy and palaeobiology of the Bathonian (Middle Jurassic) tulitid ammonite *Morrisiceras*. *Geobios* 41: 699–717. doi:10.1016/j.geobios.2007.11.001

Zatoń, M. 2007. *Ammonites from the ore-bearing clays (Bajocian–Bathonian) of the Polish Jura*. 524 pp. Unpublished Ph.D. thesis, Silesian University, Sosnowiec.

Zeiss, A. 2001. Die Ammonitenfauna der Tithonklippen von Ernstbrunn, Niederösterreich. *Neuw Denk-Schriften des Naturhistorischen Museums in Wien* 6: 1–117.

Appendix 1

Morphotype, age, source (number in square brackets), measurements and estimations of the species studied. Abbreviations: age: early (E), middle (M), and late (L), Triassic (T), Jurassic (J), and Cretaceous (C); morphotypes: Ca, cadicone; Ox, oxycone; Pl, platycone; Sp, sphaerocone; Se, serpenticone; N, number of specimens (some of them measured at different diameters); n, total number of measurements for each species. Other abbreviations and symbols as indicated in text.

Morph	Age	Species	N	n	D_{min}	D_{max}	$<H_1/D>$	$<H_2/H_1>$	$<W/D>$	$<U/D>_{obs}$	$(U/D)_{pred}$	ε (%)
Ca	LC	*Paravascoceras crassum* [1]	1	1	70.00	70.00	0.36	0.60	0.64	0.36	0.36	1
Ca	LT	*Anatropites maclearni* [2]	1	1	35.00	35.00	0.34	0.67	0.34	0.50	0.39	22
Ca	LT	*Anatropites sulfurensis* [3]	1	1	45.00	45.00	0.36	0.75	0.44	0.44	0.38	14
Ca	LT	*Hoplotropites auctus* [4]	2	2	30.00	30.00	0.38	0.66	0.55	0.35	0.33	6
Ca	MJ	*Paracadoceras efimovi* [5]	1	2	75.00	96.00	0.30	0.72	0.63	0.44	0.46	5
Ox	EC	*Barremites* gr. *difficilis* [6]	1	1	121.00	121.00	0.51	0.63	0.25	0.15	0.14	6
Ox	EC	*Grantziceras glabrum* [7]	1	1	94.00	94.00	0.49	0.61	0.30	0.15	0.17	12
Ox	EC	*Puzosia alaskana* [8]	2	2	49.00	89.00	0.55	0.67	0.29	0.13	0.11	15
Ox	EC	*Proleopoldia kurmyschensis* [9]	1	1	114.00	114.00	0.36	0.78	0.28	0.37	0.38	4
Ox	EJ	*Amaltheus bifurcus* [10]	1	1	120.00	120.00	0.37	0.82	0.19	0.38	0.38	0
Ox	EJ	*Amaltheus bondonniensis* [11]	1	1	30.00	30.00	0.37	0.73	0.23	0.37	0.36	1
Ox	EJ	*Cheltonia oustense* [12]	1	1	21.40	21.40	0.36	0.78	0.27	0.33	0.37	14
Ox	EJ	*Paroxynoticeras* aff. *subundulatum* [13]	1	1	225.00	225.00	0.44	0.61	0.26	0.22	0.24	13
Ox	EJ	*Paroxynoticeras salisburguense* [14]	1	1	152.00	152.00	0.38	0.79	0.23	0.30	0.35	17
Ox	ET	*Vavilobites obtusus* [15]	3	3	46.00	101.00	0.44	0.64	0.28	0.24	0.25	3
Ox	ET	*Vavilobites sverdrupi* [16]	2	3	78.00	151.00	0.47	0.66	0.15	0.22	0.20	9
Ox	ET	*Vishnuites pralamha* [17]	1	1	55.00	55.00	0.40	0.68	0.16	0.36	0.31	15
Ox	ET	*Wordioceras wordiei* [18]	4	4	28.00	124.00	0.40	0.72	0.24	0.33	0.32	4
Ox	ET	*Arctoprionites prontschischevi* [19]	1	1	32.00	32.00	0.47	0.60	–	0.16	0.19	24
Ox	ET	*Nordophiceras schmidti* [20]	1	1	38.00	38.00	0.45	0.71	–	0.24	0.25	4
Ox	ET	*Otoceras woodwardi* [21]	2	2	41.00	70.00	0.48	0.68	0.38	0.19	0.20	5
Ox	LC	*Metengonoceras aspenanum* [22]	3	3	26.00	75.00	0.56	0.59	0.20	0.05	0.06	20
Ox	LC	*Metengonoceras taigeense* [23]	3	3	90.00	168.00	0.55	0.55	0.16	0.06	0.06	3
Ox	LJ	*Neocampylites henrici* [24]	1	1	110.00	110.00	0.56	0.66	0.35	0.11	0.09	16
Ox	LJ	*Ochetoceras canaliculatum* [25]	1	1	55.00	55.00	0.52	0.68	0.31	0.12	0.14	12
Ox	LT	*Dryojuvavites ochardi* [26]	1	1	52.00	52.00	0.50	0.62	0.42	0.13	0.15	14
Ox	LT	*Parajuvavites canadensis* [27]	3	3	43.00	52.00	0.44	0.62	0.30	0.16	0.23	46
Ox	MJ	*Dundryites* aff. *albidus* [28]	1	1	149.00	149.00	0.47	0.69	0.22	0.22	0.21	4
Ox	MT	*Amphipopanoceras selwyni* [29]	2	2	58.00	61.00	0.42	0.58	0.27	0.25	0.26	6

doi:10.4202/app.2009.0066

Morph	Age	Species	N	n	D_{min}	D_{max}	$<H_1/D>$	$<H_2/H_1>$	$<W/D>$	$<U/D>_{obs}$	$(U/D)_{pred}$	ε (%)
Ox	MT	*Amphipopanoceras tetsa* [30]	3	3	24.00	70.00	0.48	0.55	0.36	0.16	0.17	2
Ox	MT	*Stenopopanoceras angulatum* [31]	2	2	33.00	44.00	0.38	0.65	0.26	0.32	0.34	6
Ox	MT	*Timites variabilis* [32]	1	1	35.30	35.30	0.53	0.54	0.32	0.08	0.09	22
Pl	EC	*Emerisiceras* aff. *irigoyeni* [33]	1	1	160.00	160.00	0.41	1.06	0.34	0.36	0.36	2
Pl	EC	*Emerisiceras* gr. *barremense* [34]	1	1	133.00	133.00	0.35	1.13	0.30	0.43	0.44	4
Pl	EC	*Emerisiceras hammatoptychum* [35]	1	1	119.00	119.00	0.36	1.05	0.30	0.40	0.41	5
Pl	EC	*Emerisiceras magnini* [36]	4	4	105.00	195.00	0.39	1.03	0.24	0.38	0.37	2
Pl	EC	*Emerisiceras murphyi* [37]	1	1	76.00	76.00	0.42	1.06	0.30	0.36	0.35	3
Pl	EC	*Hemihoplites astarte* [38]	3	3	106.00	143.00	0.35	0.91	0.28	0.40	0.41	3
Pl	EC	*Hemihoplites soulieri* [39]	2	2	90.00	102.00	0.38	0.90	0.14	0.35	0.37	5
Pl	EC	*Arcthoplites talkeetnatus* [40]	5	5	28.50	180.00	0.44	0.69	0.30	0.26	0.26	1
Pl	EC	*Brewericeras hulenense* [41]	1	1	97.00	97.00	0.45	0.80	0.24	0.21	0.26	24
Pl	EC	*Freboldiceras singulare* [42]	2	2	52.00	58.00	0.43	0.64	0.33	0.27	0.26	4
Pl	EC	*Eotetragonites gainesi* [43]	2	2	58.00	66.00	0.44	0.75	0.18	0.29	0.26	9
Pl	EC	*Malbosiceras malbosi* [44]	2	2	83.00	102.00	0.33	0.83	0.29	0.43	0.42	0
Pl	EC	*Malbosiceras tarini* [45]	2	2	69.00	79.00	0.36	0.87	0.34	0.39	0.39	2
Pl	EC	*Heinzia provincialis* [46]	1	1	44.00	44.00	0.45	0.75	0.32	0.23	0.25	8
Pl	EC	*Kosmatella cappsi* [47]	1	1	70.00	70.00	0.43	0.77	0.33	0.29	0.28	1
Pl	EJ	*Aegoceras lataecostata* [48]	1	1	66.00	66.00	0.30	0.90	0.27	0.47	0.48	2
Pl	EJ	*Androgynoceras* aff. *sparsicosta* [49]	1	1	28.00	28.00	0.32	0.78	0.36	0.39	0.44	11
Pl	EJ	*Epideroceras* cf. *ponticum* [50]	1	1	144.00	144.00	0.37	0.72	0.33	0.35	0.36	2
Pl	EJ	*Platypleuroceras brebispinum* [51]	1	1	72.00	72.00	0.26	0.89	0.19	0.54	0.53	1
Pl	EJ	*Uptonia jamesoni* [52]	1	1	106.00	106.00	0.29	0.87	0.14	0.46	0.49	6
Pl	EJ	*Galaticeras aegoceroides* [53]	1	1	19.00	19.00	0.43	0.76	0.30	0.30	0.28	7
Pl	EJ	*Gorgheiceras costotuberculatum* [54]	1	1	15.00	15.00	0.44	0.72	–	0.30	0.26	12
Pl	EJ	*Zaghouanites arcanum* [55]	1	1	64.00	64.00	0.41	0.77	0.33	0.32	0.30	5
Pl	EJ	*Zaghouanites bettonii* [56]	1	1	24.60	24.60	0.42	0.82	0.30	0.29	0.30	4
Pl	EJ	*Tragophylloceras loscombi* [57]	1	1	71.00	71.00	0.55	0.69	0.23	0.13	0.11	13
Pl	EJ	*Tragophylloceras multicostatum* [58]	2	2	30.00	63.00	0.45	0.69	0.31	0.25	0.24	0
Pl	EJ	*Jamesonites spoliatus* [59]	2	2	56.00	100.00	0.34	0.85	0.23	0.41	0.42	2
Pl	EJ	*Paracymbites dennyiformis* [60]	1	1	17.00	17.00	0.41	0.74	0.18	0.25	0.30	20
Pl	EJ	*Parasteroceras rakusi* [61]	1	1	98.20	98.20	0.37	0.73	0.18	0.34	0.35	3
Pl	EJ	*Protocymbites*? *azzouzi* [62]	1	1	16.00	16.00	0.46	0.59	0.34	0.25	0.21	16
Pl	EJ	*Tropidoceras flandrini* [63]	2	2	103.40	146.00	0.38	0.85	0.18	0.38	0.37	5
Pl	ET	*Ophiceras commune* [64]	1	1	55.00	55.00	0.40	0.77	0.22	0.29	0.32	11
Pl	ET	*Ophiceras medium* [65]	4	4	48.00	59.00	0.38	0.72	0.22	0.30	0.34	11
Pl	ET	*Wasatchites deleeni* [66]	4	4	32.00	51.00	0.43	0.69	0.30	0.25	0.27	5
Pl	LC	*Nigericeras jacketi* [67]	2	2	54.00	93.00	0.50	0.66	0.39	0.16	0.17	3
Pl	LC	*Paramammites subconciliatus* [68]	4	4	26.00	105.00	0.42	0.64	0.50	0.25	0.27	8
Pl	LC	*Pseudaspidoceras paganum* [69]	1	1	163.00	163.00	0.36	0.75	0.37	0.40	0.37	6
Pl	LC	*Pseudotissotia nigeriensis* [70]	6	6	42.00	185.00	0.52	0.62	0.41	0.14	0.12	11
Pl	LC	*Romaniceras mexicanum* [71]	5	5	46.00	207.00	0.42	0.92	0.45	0.31	0.32	2
Pl	LC	*Spathites rioensis* [72]	2	2	45.00	53.00	0.53	0.62	0.42	0.14	0.11	22
Pl	LC	*Tarrantoceras sellardsi* [73]	3	3	52.00	83.00	0.38	0.85	0.34	0.33	0.37	10
Pl	LC	*Kossmaticeras centinelaense* [74]	2	2	81.00	104.00	0.39	0.75	0.30	0.30	0.33	10
Pl	LC	*Exiteloceras jenneyi* [75]	3	3	83.00	193.00	0.26	1.54	0.20	0.57	0.58	3
Pl	LJ	*Creniceras renggeri* [76]	10	10	9.90	21.30	0.48	0.75	0.28	0.19	0.21	8
Pl	LJ	*Hecticoceras kersteni* [77]	5	5	5.90	40.70	0.45	0.84	0.26	0.30	0.27	11
Pl	LJ	*Hecticoceras schumacheri* [78]	34	34	3.30	33.70	0.40	0.84	0.32	0.36	0.34	6
Pl	LJ	*Hecticoceras socini* [79]	52	52	3.80	37.30	0.41	0.86	0.32	0.34	0.32	5
Pl	LJ	*Lissoceratoides erato* [80]	3	3	9.50	52.00	0.47	0.81	0.29	0.27	0.24	13
Pl	LJ	*Pseudolissoceras zitteli* [81]	16	22	15.00	138.00	0.48	0.74	0.31	0.20	0.21	9
Pl	LJ	*Choicensisphinctes* sp. [82]	2	2	37.00	41.50	0.42	0.80	0.32	0.27	0.30	11
Pl	LJ	*Euaspidoceras hypselum* [83]	3	4	8.80	113.00	0.38	0.93	0.51	0.36	0.37	2
Pl	LJ	*Gravesia gravesiana* [84]	3	3	315.00	367.00	0.32	0.74	0.35	0.40	0.43	8
Pl	LJ	*Lithacoceras* aff. *malarguense* [85]	5	9	33.30	184.00	0.35	0.76	0.32	0.40	0.39	2
Pl	LJ	*Zittelia eudichtoma* [86]	2	2	66.00	68.00	0.31	0.85	0.30	0.44	0.47	6
Pl	LT	*Alloclionites dieneri* [87]	2	2	54.00	71.00	0.42	0.75	0.38	0.32	0.29	7
Pl	LT	*Eotetidites lacrimosus* [88]	2	2	27.00	95.00	0.30	0.84	0.38	0.46	0.47	2
Pl	LT	*Leislinghites politus* [89]	2	2	23.00	29.00	0.37	0.74	0.39	0.35	0.36	4
Pl	LT	*Simpolycyclus gunningi* [90]	1	1	17.00	17.00	0.35	0.83	0.35	0.38	0.40	4
Pl	LT	*Discotropites smithi* [91]	1	1	26.00	26.00	0.54	0.86	0.38	0.19	0.17	11
Pl	MJ	*Hecticoceras* sp. [92]	5	5	3.12	17.58	0.40	0.84	0.33	0.33	0.34	0

Morph	Age	Species	N	n	D_{min}	D_{max}	$<H_1/D>$	$<H_2/H_1>$	$<W/D>$	$<U/D>_{obs}$	$(U/D)_{pred}$	ε (%)
Pl	MJ	*Witchellia romanoides* [93]	1	1	90.00	90.00	0.39	0.73	0.20	0.36	0.33	9
Pl	MJ	*Procerites arkelli* [94]	5	6	70.00	222.00	0.42	0.62	0.30	0.27	0.28	2
Pl	MT	*Anagymnotoceras spivaki* [95]	1	1	53.00	53.00	0.49	0.73	0.33	0.20	0.19	2
Pl	MT	*Ceratites enodis* [96]	2	2	78.00	84.00	0.38	0.71	–	0.31	0.34	10
Pl	MT	*Ceratites evolutus* [97]	1	1	79.00	79.00	0.39	0.74	–	0.33	0.33	0
Pl	MT	*Ceratites obesus* [98]	2	2	65.00	90.00	0.44	0.69	–	0.24	0.25	5
Pl	MT	*Ceratites pendorfi* [99]	3	3	92.00	101.00	0.41	0.73	–	0.31	0.31	1
Pl	MT	*Ceratites praecursor* [100]	1	1	77.00	77.00	0.36	0.79	–	0.34	0.38	12
Pl	MT	*Ceratites spinosus* [101]	1	1	61.00	61.00	0.43	0.73	–	0.30	0.28	5
Pl	MT	*Eogymnotoceras janvieri* [102]	3	3	25.00	34.00	0.37	0.86	0.31	0.40	0.38	5
Pl	MT	*Eogymnotoceras tuberculatum* [103]	2	2	37.00	99.00	0.46	0.73	0.28	0.27	0.24	10
Pl	MT	*Praeczekanowskites tumaefactus* [104]	3	3	33.60	45.50	0.50	0.52	0.44	0.21	0.13	39
Se	EC	*Acrioceras ornatum alpinum* [105]	1	1	49.00	49.00	0.34	1.47	–	0.47	0.53	12
Se	EC	*Aegocrioceras quadratum* [106]	1	1	94.70	94.70	0.24	1.23	–	0.56	0.59	5
Se	EC	*Crioceratites* aff. *majoricensis* [107]	6	6	39.00	88.00	0.29	1.40	0.17	0.53	0.54	3
Se	EC	*Crioceratites apricus* [108]	1	1	81.00	81.00	0.32	1.21	0.31	0.46	0.48	6
Se	EC	*Crioceratites* cf. *schlagintweiti* [109]	1	1	88.00	88.00	0.32	1.18	0.30	0.47	0.48	2
Se	EC	*Crioceratites curnieri* [110]	4	4	49.00	68.00	0.27	1.29	0.16	0.54	0.56	4
Se	EC	*Crioceratites dilatatum* [111]	2	2	66.00	95.00	0.32	1.37	0.19	0.49	0.50	2
Se	EC	*Crioceratites nolani* [112]	13	13	53.00	99.00	0.28	1.51	0.17	0.54	0.56	4
Se	EC	*Crioceratites quenstedti* [113]	1	1	52.00	52.00	0.31	1.19	0.18	0.50	0.50	1
Se	EC	*Crioceratites schlagintweiti* [114]	1	1	183.00	183.00	0.28	1.24	0.26	0.51	0.54	5
Se	EC	*Crioceratites sornayi* [115]	5	5	58.00	95.00	0.27	1.49	0.16	0.56	0.57	1
Se	EC	*Emerisiceras*? sp. [116]	3	3	71.00	173.00	0.34	1.12	–	0.44	0.45	2
Se	EC	*Peltocrioceras deeckei* [117]	1	1	205.00	205.00	0.33	1.30	0.30	0.51	0.48	6
Se	EC	*Protacrioceras ornatum* [118]	4	4	47.00	84.00	0.30	1.59	0.18	0.52	0.54	5
Se	EC	*Tropaeum magnum* [119]	1	1	495.00	495.00	0.35	1.26	0.35	0.41	0.45	11
Se	EC	*Eogaudryceras hertleini* [120]	2	2	48.00	49.00	0.42	0.78	0.37	0.30	0.29	3
Se	EC	*Eogaudryceras numidum* [121]	1	1	69.00	69.00	0.42	0.79	0.43	0.32	0.30	6
Se	EC	*Gaudryceras* sp. [122]	1	1	37.00	37.00	0.41	0.73	0.62	0.32	0.31	5
Se	EC	*Anagaudryceras aurarium* [123]	1	1	49.00	49.00	0.43	0.86	0.43	0.33	0.30	8
Se	EJ	*Dactylioceras clevelandicum* [124]	3	3	74.00	81.00	0.24	0.85	0.31	0.57	0.57	0
Se	EJ	*Perilytoceras denckmanni* [125]	1	1	312.00	312.00	0.47	0.72	0.33	0.28	0.22	23
Se	EJ	*Perilytoceras jurense* [126]	2	2	140.00	142.70	0.43	0.86	0.37	0.30	0.29	1
Se	EJ	*Acanthopleuroceras solare* [127]	2	2	59.00	67.00	0.26	0.89	0.20	0.52	0.54	3
Se	EJ	*Neophyllites neumayri* [128]	1	1	38.00	38.00	0.29	0.73	0.18	0.45	0.48	8
Se	ET	*Paranannites spathi* [129]	2	2	32.00	32.00	0.41	0.50	0.58	0.30	0.27	9
Se	ET	*Olenekoceras mittendorffi* [130]	1	1	53.00	53.00	0.38	0.70	–	0.36	0.35	4
Se	ET	*Olenikites spiniplicatus* [131]	2	2	28.50	29.00	0.35	0.70	–	0.38	0.39	2
Se	ET	*Hypophiceras gracile* [132]	1	1	36.00	36.00	0.25	1.00	0.19	0.53	0.56	7
Se	ET	*Kashmirites warreni* [133]	4	4	36.00	62.00	0.28	0.82	0.21	0.52	0.50	4
Se	ET	*Tompophiceras extremum* [134]	2	2	46.00	60.00	0.26	0.93	0.23	0.50	0.54	9
Se	LJ	*Lytoceras* aff. *montanum* [135]	1	1	80.00	80.00	0.33	0.92	–	0.48	0.45	6
Se	LJ	*Lytoceras* aff. *municipalis* [136]	1	1	166.00	166.00	0.34	0.95	0.35	0.45	0.43	5
Se	LJ	*Catutosphinctes araucanensis* [137]	2	2	53.40	192.00	0.31	0.79	0.33	0.47	0.45	3
Se	LJ	*Catutosphinctes proximus* [138]	2	7	6.20	66.10	0.34	0.80	0.42	0.44	0.41	8
Se	LJ	*Catutosphinctes* sp. [139]	2	2	38.50	41.00	0.29	0.85	0.29	0.47	0.49	4
Se	LJ	*Choicensisphinctes* cf. *limits* [140]	3	5	141.50	310.00	0.38	0.77	0.36	0.34	0.35	1
Se	LJ	*Cordubiceras gemmatum* [141]	2	2	89.00	99.00	0.27	1.00	0.11	0.51	0.53	5
Se	LJ	*Djurjuriceras mutari* [142]	3	3	117.00	173.00	0.30	0.92	–	0.49	0.48	1
Se	LJ	*Micracanthoceras rodhanicum* [143]	2	2	59.00	61.00	0.26	0.84	0.23	0.54	0.54	0
Se	LJ	*Perisphinctes bernensis* [144]	67	67	3.50	40.90	0.37	0.63	0.60	0.34	0.34	2
Se	LJ	*Perisphinctes paneaticus* [145]	41	41	4.80	23.90	0.39	0.84	0.54	0.35	0.34	1
Se	LJ	*Perisphinctes vicinus* [146]	36	36	4.40	50.70	0.35	0.74	0.48	0.40	0.39	2
Se	LJ	*Windhauseniceras internispinosum* [147]	4	5	60.70	199.00	0.32	0.85	0.33	0.46	0.45	3
Se	LT	*Choristoceras shoshonensis* [148]	2	2	24.00	29.00	0.25	1.07	0.27	0.53	0.57	9
Se	LT	*Vandaites neoyorkensis* [149]	1	1	32.00	32.00	0.28	1.11	0.22	0.53	0.53	1
Se	MJ	*Bajocia farcyi* [150]	3	3	15.50	18.00	0.19	0.90	0.21	0.64	0.65	2
Se	MJ	*Binatisphinctes mosquensis* [151]	6	6	3.57	14.97	0.29	0.91	0.39	0.49	0.50	2
Se	MJ	*Choffattia* aff. *neumayri* [152]	9	9	82.00	31.00	0.31	0.78	0.31	0.45	0.45	2
Se	MJ	*Kosmoceras* sp. [153]	5	5	3.70	10.93	0.34	0.81	0.54	0.42	0.41	2
Se	MJ	*Polysphinctites tenuiplicatus* [154]	23	55	7.00	98.90	0.34	0.81	0.28	0.45	0.42	8
Se	MJ	*Parapatoceras distans* [155]	4	4	7.20	29.00	0.24	1.44	–	0.61	0.60	2

doi:10.4202/app.2009.0066

Morph	Age	Species	N	n	D_{min}	D_{max}	$<H_1/D>$	$<H_2/H_1>$	$<W/D>$	$<U/D>_{obs}$	$(U/D)_{pred}$	ε (%)
Se	MJ	*Spiroceras annulatum* [156]	1	1	16.00	16.00	0.34	1.09	–	0.44	0.44	1
Se	MJ	*Spiroceras orbignyi* [157]	5	7	20.00	37.00	0.21	1.88	–	0.68	0.66	3
Se	MJ	*Emileia* aff. *dundriensis* [158]	1	1	262.00	262.00	0.25	0.82	0.26	0.53	0.55	3
Se	MT	*Nicholsites parisi* [159]	1	1	68.00	68.00	0.49	0.64	0.26	0.21	0.18	13
Sp	EC	*Moffitites robustus* [160]	3	3	45.00	61.00	0.41	0.67	0.67	0.29	0.30	3
Sp	EC	*Olcostephanus mingrammi* [161]	3	3	56.00	76.00	0.36	0.77	0.53	0.39	0.38	2
Sp	EC	*Olcostephanus permolestus* [162]	4	4	26.00	49.00	0.38	0.73	0.22	0.37	0.35	5
Sp	EC	*Polyptychites keyserlingi* [163]	1	1	107.00	107.00	0.37	0.63	0.50	0.31	0.34	10
Sp	EC	*Polyptychites pavlowi* [164]	1	1	101.30	101.30	0.38	0.62	0.39	0.32	0.33	3
Sp	EC	*Polyptychites stubendorffi* [165]	1	1	71.00	71.00	0.43	0.42	0.52	0.27	0.21	20
Sp	EJ	*Liparoceras gallicum* [166]	1	1	177.00	177.00	0.55	0.73	0.50	0.13	0.12	5
Sp	EJ	*Frechiella subcarinata* [167]	3	3	37.00	88.50	0.49	0.77	0.55	0.22	0.20	8
Sp	LC	*Paravascoceras carteri* [168]	1	1	108.00	108.00	0.37	0.45	0.76	0.35	0.32	9
Sp	LC	*Paravascoceras nigeriense* [169]	1	1	99.00	99.00	0.42	0.60	0.45	0.24	0.26	7
Sp	LC	*Paravascoceras tectiforme* [170]	3	3	80.00	135.00	0.45	0.63	0.62	0.22	0.22	2
Sp	LC	*Tomasites gongilensis* [171]	2	2	59.00	94.00	0.47	0.61	0.55	0.20	0.20	1
Sp	LC	*Vascoceras costatum* [172]	5	5	38.00	115.00	0.42	0.66	0.51	0.27	0.28	4
Sp	LJ	*Scaphitodites scaphitoides* [173]	37	37	5.50	14.10	0.48	0.68	0.43	0.17	0.20	16
Sp	LJ	*Taramelliceras hermonis* [174]	65	65	4.70	39.60	0.54	0.71	0.39	0.15	0.12	19
Sp	LJ	*Taramelliceras richei* [175]	61	61	5.10	15.70	0.54	0.71	0.34	0.15	0.13	16
Sp	LJ	*Aspidoceras* cf. *euomphalum* [176]	1	1	125.00	125.00	0.46	0.84	0.61	0.27	0.26	3
Sp	LJ	*Pseudhimalayites* cf. *steinmanni* [177]	1	1	438.00	438.00	0.41	0.87	0.53	0.30	0.33	7
Sp	LJ	*Callyphyllocerals schems* [178]	13	13	4.80	59.30	0.49	0.72	0.39	0.23	0.19	15
Sp	LT	*Juvavites concretus* [179]	1	1	84.00	84.00	0.52	0.55	0.40	0.12	0.10	14
Sp	LT	*Juvavites levigatus* [180]	1	1	70.00	70.00	0.49	0.44	0.40	0.13	0.13	3
Sp	MJ	*Poecilomorphus cycloides* [181]	6	6	13.50	17.50	0.46	0.73	0.41	0.26	0.24	6
Sp	MJ	*Bullatimorphites* sp. [182]	1	1	46.20	46.20	0.55	0.43	1.14	0.05	0.04	26
Sp	MJ	*Morrisiceras morrisi* [183]	45	57	4.50	200.00	0.44	0.69	0.62	0.25	0.25	0
Sp	MJ	*Ptychophylloceras flabellatum* [184]	1	1	88.00	88.00	0.54	0.57	0.35	0.10	0.08	23
Sp	MJ	*Ptychophylloceras haloricum* [185]	1	1	84.00	84.00	0.54	0.58	0.36	0.11	0.09	12
Sp	MJ	*Emileia malenotata* [186]	1	1	49.00	49.00	0.41	0.60	0.45	0.31	0.28	7
Sp	MJ	*Eurycephalites extremus* [187]	4	4	8.30	99.90	0.47	0.57	0.67	0.16	0.19	21
Sp	MJ	*Eurycephalites gottschei* [188]	40	69	3.80	80.30	0.48	0.56	0.62	0.13	0.17	27
Sp	MJ	*Eurycephalites rotundus* [189]	7	11	3.10	37.00	0.49	0.62	0.57	0.14	0.17	25
Sp	MJ	*Kepplerites keppleri* [190]	3	3	60.00	126.00	0.41	0.65	0.41	0.29	0.29	3
Sp	MJ	*Lilloettia steinmanni* [191]	5	5	10.00	60.50	0.52	0.60	0.61	0.12	0.12	1
Sp	MJ	*Macrocephalites chrysoolithicus* [192]	1	7	3.70	246.00	0.45	0.65	0.73	0.21	0.23	9
Sp	MJ	*Macrocephalites compressus* [193]	1	5	3.50	79.20	0.47	0.66	0.55	0.23	0.21	11
Sp	MJ	*Macrocephalites herveyi* [194]	1	7	3.78	111.00	0.41	0.61	0.66	0.34	0.29	14
Sp	MJ	*Macrocephalites macrocephalus* [195]	1	6	3.52	156.10	0.47	0.66	0.52	0.21	0.21	3
Sp	MJ	*Otoites* sp. [196]	1	5	4.30	50.30	0.43	0.63	0.72	0.24	0.26	7
Sp	MJ	*Quenstedtoceras lamberti* [197]	6	6	192.00	228.00	0.43	0.71	0.60	0.26	0.27	2
Sp	MJ	*Stehnocephalites crassicostatus* [198]	7	7	40.00	106.90	0.42	0.62	0.49	0.26	0.27	2
Sp	MJ	*Stehnocephalites gerthi* [199]	53	146	3.60	134.50	0.44	0.57	0.62	0.21	0.23	8
Sp	MT	*Ceratites dorsoplanatus* [200]	1	1	120.00	120.00	0.44	0.66	–	0.21	0.25	18
Sp	MT	*Ceratites flexuosus* [201]	1	1	84.00	84.00	0.46	0.74	–	0.24	0.23	3

1, 67–71: Meister (1989); 2–4, 15–18, 26–31, 64, 66, 87–91, 129, 132–134, 179–180: Tozer (1994); 5: Gulyaev (2001); 7, 40–41: Jones (1967); 8, 42, 47, 123, 160: Imlay (1960); 9, 190: Mitta and Starodubtseva (2000); 10–11, 48–49, 52, 166: Meister (1986); 12–14, 53–56, 60–62: Rakus and Guex (2002); 17, 21, 65: Kummel (1972); 19–20, 130–131: Zakharov and Schkolnik (1994); 22–23: Cobban and Kennedy (1989); 24–25: Branger et al. (1995); 6, 33–39, 46, 116: Delanoy (1992); 43, 120–122: Murphy (1967); 44–45, 86, 141–143: Tavera (1985); 50–51: Dommergues (1987); 57–58: Joly (2000); 59, 63, 127: Schlatter (1980); 71: Kennedy and Cobban (1988); 72: Cobban (1988b); 73: Cobban (1988a); 74: Riccardi (1983); 75: Kennedy et al. (2000); 76–80, 144–146, 173–175, 178: Haas (1955); 24–25, 82–83, 85, 137–140, 176–177, 196: collection LPB; 84: collection Armin Scherzinger, Hattingen, Germany; 92, 151, 153: Sprey (2002); 94: Pandey and Callomon (1995); 95, 102–103, 159: Bucher (1994); 96–101, 200–201: Ulrichs (2006); 32, 104: Dagys (2001); 105: Patrulius and Avram (1976); 106, 163–165: Kemper and Wiedenroth (1987); 107, 110, 112, 115, 118: Ropolo and Salomon (1992); 108: Giovine (1952); 109, 114: Giovine (1950); 111, 113: Ropolo and Gonnet (1995); 117, 119: Aguirre-Urreta (1985); 124: Howarth (1973); 125–126: Rulleau (1997); 128: Bloos (2004); 135–136: Zeiss (2001); 147: collection MOZ–PI; 148–149: Taylor and Guex (2002); 150, 181: Sturani (1971); 152, 187, 189, 191, 198–199: Parent (1998); 154: Zatoń (2007); 155–157: Dietl (1978); 28, 93, 158, 186: Dietze et al. (2007); 161–162: Aguirre-Urreta and Rawson (1999); 167: Rulleau et al. (2003); 182: Burckhardt (1927); 183: Zatoń (2008); 184–185: Pavia (1983); 188: Parent (1997); 192–195: Thierry (1978); 197: Callomon (1985).